IOP Publishing Measurement Science and Technology
Meas. Sci. Technol. **31** (2020) 054007 (9pp) https://doi.org/10.1088/1361-6501/ab64ac

Phosphor thermometry instrumentation for synchronized acquisition of luminescence lifetime decay and intensity on thermal barrier coatings

Quentin Fouliard[1], Johnathan Hernandez[1], Bauke Heeg[2], Ranajay Ghosh[1] and Seetha Raghavan[1]

[1] University of Central Florida, 4000 Central Florida Blvd., Orlando, FL 32816, United States of America
[2] Lumium, Eewal 84, 8911 GV Leeuwarden, The Netherlands

E-mail: seetha.raghavan@ucf.edu

Received 8 October 2019, revised 20 November 2019
Accepted for publication 20 December 2019
Published 26 February 2020

Abstract

Thermal barrier coatings (TBCs) are used to protect turbine components from extreme environments and to allow for the turbine system to operate at temperatures beyond the melting point of the underlying superalloy blade. Existing *in situ* temperature measurement methods for high temperature evaluation have inherent uncertainties that impose important safety margins. Improving the accuracy of temperature measurements on the materials in operating conditions is key for more reliable lifetime predictions and to increase turbine system efficiencies. For this objective, phosphor thermometry shows great potential for non-invasive high temperature measurements on luminescent coatings. In this work, a phosphor thermometry instrument has been developed to collect two emission peaks simultaneously of an erbium and europium co-doped yttria-stabilized zirconia TBC, enabling an extended temperature range and high precision of the *in situ* temperature assessment. The luminescence lifetime decays and the intensity variations of both dopants were captured by the instrument, testing its high sensitivity and extended temperature range capabilities for accurate measurements, up to operating temperatures for turbine engines. The results open the way for the applicability of portable phosphor thermometry instrumentation to perform effective temperature monitoring on turbine engine materials and support the advancement of innovative sensing coatings.

Keywords: phosphor thermometry, thermal barrier coatings, erbium europium co-doped yttria-stabilized zirconia, luminescence decay, intensity ratio

(Some figures may appear in colour only in the online journal)

1. Introduction

Thermal barrier coatings are widely used in turbine systems to protect the components operating at high temperatures. They are generally used in combination with active cooling systems that allow for temperature drops through the ceramic top coat, in the order of 1 °C μm^{-1} [1, 2]. Accurate measurement of coating temperatures in such extreme environments is crucial to ensure and maintain good performance, functionality of the system, and predictions on the lifetime of the turbine blades. The temperature measurement uncertainty has to be reduced to a few degrees at service temperatures as failure mechanisms are thermally driven. This is particularly important due to the extreme sensitivity of the growth rate of the thermally grown oxide to the temperature at the interface between the top coat and the bond coat [3–5]. Currently, the viable techniques for

non-contact *in situ* temperature measurements are infrared thermometry, for which precision is limited by the presence of emissions from the operation of the turbine engines, as well as emissivity variation, and phosphor thermometry, which shows potential as a reliable method for precision temperature measurements [6, 7]. Phosphor thermometry has proven to be effective at high temperatures using rare-earth or transition metal-doped ceramics that can be embedded into TBC configurations to enable real-time temperature monitoring in service conditions [8–13]. Among the possible sensors for high temperature measurements integrated into TBCs, rare-earth doped yttria-stabilized zirconia (YSZ:RE) have been largely studied as they offer sensing capabilities with ease of integration in existing standard TBCs and no layer compatibility mismatches. Particularly, europium-doped YSZ (YSZ:Eu^{3+}) has been extensively selected as it has excellent temperature sensitivity past its quenching temperature of about 500 °C [14] and an intense visible luminescence with a long room temperature decay time [15, 16]. Similarly, erbium-doped YSZ (YSZ:Er^{3+}) has a strong visible luminescence intensity [17]. It has a shorter room temperature decay time and a temperature sensitivity on the entire range between room temperature and turbine operating temperatures [18]. Having a usable absorption band at 532 nm [19] and distinct emission wavelengths, both dopants can be used together in a co-doped configuration that possesses their combined properties. The two dopants have been used together in literature in a YSZ host for multi-layer rainbow sensors [20], thermal history sensors [19, 21], and in Y_2O_3 for intensity ratio measurements [22]. In this work, instrumentation was developed so that the luminescence produced by YSZ:Er^{3+} and YSZ:Eu^{3+} could be isolated and simultaneously collected with the objective of doubling the data for higher precision, combining sensitivities of the dopants and extending the temperature range at which the instrument can measure *in situ* temperature on rare-earth doped YSZ TBCs. The decay and intensity ratio methods were used jointly, as reported in literature [23, 24], to take advantage of the synchronized collection of two dopants. The sample contains the sensing layer at its top surface so the phosphor thermometry measurement can be compared with infrared thermometry. Additionally, this configuration allows for the strongest luminescence intensity to emerge out of the sample [25].

2. Materials and manufacturing

2.1. Description of the fabrication process

The sample was fabricated using an SGT-100 (Praxair) spray gun at the air plasma spray (APS) facility of the Florida Institute of Technology. The materials and parameters used for the deposition of the layered configuration are given in table 1. The substrate is a 25.4 mm diameter and 3 mm thickness CM247 disk. The sample was grit blasted prior to the deposition of the bond coat layer. A stud was welded on the back of the substrate to mount the sample on the deposition stage. NiCrAlY bond coat powder (NI-164/NI-211, Praxair), 7–8 wt.% YSZ undoped top coat powder (ZRO-271, Praxair) and erbium- and europium-doped YSZ top coat powders (produced by the solid state reaction by Phosphor Technology Ltd.) were used for the deposition of the layers, as shown in figure 1(a). The erbium concentration of 1.5 wt.% in YSZ was chosen for optimal luminescence intensity, based on literature [20]. The europium concentration of 3 wt.% was chosen for high luminescence intensity and limited dopant intrusiveness to prevent from phase change [26]. As the preprocessing doped YSZ powders had initially a smaller particle size ($D_{50} < 1$ μm) and irregular particle shapes, they were mixed together with the undoped YSZ powder to ensure the flowability of the mixture and a good deposition rate for the uppermost layer. The feeding wheel speed was decreased to get a constant deposition rate with reduced clogging probability of the APS system. It was found that a mixing ratio of 1:2 for the doped powder in undoped powder was optimal to get a good deposition rate while keeping sufficient doped material for luminescence intensity. The fabricated TBC was examined using scanning electron microscopy, as presented in figure 1(b), with secondary electrons and an accelerating voltage of 15 kV. The uninterrupted and successive deposition of undoped and doped YSZ layers ensured the uniformity of the overall top coat with no visible interface. The sample was annealed for 2 h at 800 °C to remove potentially present luminescence quenching compounds.

2.2. Spectral characterization of the sample

The emission spectrum of the YSZ:Er,Eu sample has been measured with a collection time of 1 ms using a fiber collection spectrometer (Pixis 100, Princeton Instruments) under a 15 mW 532 nm laser excitation. The probe has a focal length of 7.5 mm, a depth of field of 2.2 mm, a numerical aperture of 0.27, and a spot size of 200 μm. The Er-lines at 545 nm and 562 nm and the Eu-lines at 590 nm and 606 nm were observed. The co-doping might introduce some level of re-absorption of the erbium lines due to the presence of europium that possesses an absorption band that excites the $^5D_1$ level and that extends from 520 to 550 nm [15, 27]. This could ultimately result in a smaller intensity ratio between erbium and europium. For this study, the peak of erbium at 545 nm ($^4S_{3/2} \rightarrow {}^4I_{15/2}$) and the peak of europium at 590 nm ($^5D_0 \rightarrow {}^7F_1$) were chosen for luminescence intensity and decay measurements. Figure 2 shows the emission spectrum of the YSZ:Er,Eu sample, highlighting the two regions that were collected by the phosphor thermometry detectors.

3. Phosphor thermometry system characteristics

3.1. General specifications of the instrument

The phosphor thermometry system that is presented in figure 3 has been constructed so it is adaptable to any temperature sensor that has at least two emission peaks that can be isolated by means of dichroic filters. The instrument was also made portable by setting up the system on a stable cart for which the height can be adjusted by either lifting the top surface of the cart or individually lifting the photomultiplier tubes (PMTs) as they are mounted on precision lab lift jacks, fixed on the main

Table 1. Materials and parameters for the air plasma spray deposition.

Layer	Bond coat	Undoped top coat	Doped top coat
Material (Mixing percentages, given in wt. %)	NiCrAlY	YSZ	66% YSZ + 17% YSZ:Er (1.5% Er) + 17% YSZ:Eu (3% Eu)
Thickness (µm)	150	250	80
Spray distance (cm)	10	7.5	7.5
Current (A)	802	902	902
Voltage (V)	43.3	43.7	43.7
Argon (SLM)	49.1	25.5	25.5
Helium (SLM)	20.3	20.8	20.8
Feeding wheel speed (rpm)	1.17	3.29	0.48

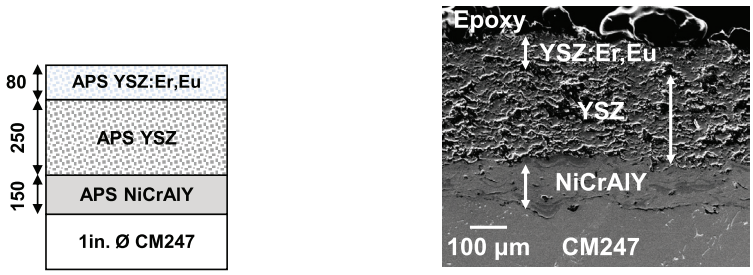

(a) (b)

Figure 1. APS TBC configuration including a luminescent layer of YSZ:Er,Eu. (a) TBC sample layer configuration. Units in µm. (b) TBC sample microstructure.

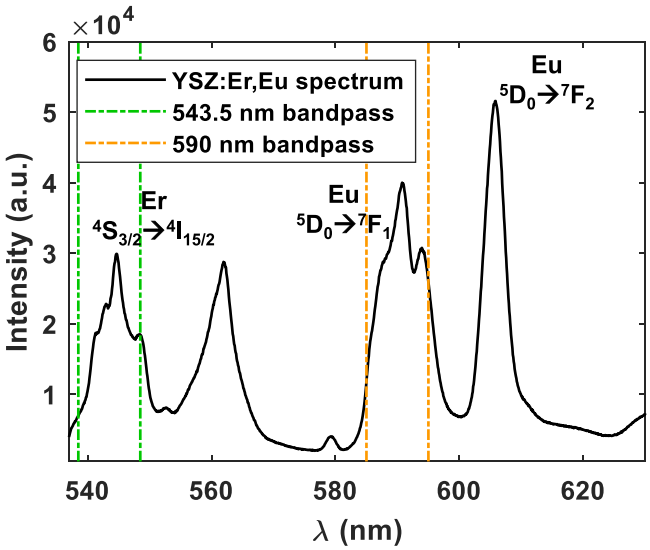

Figure 2. Emission spectrum of YSZ:Er,Eu under 532 nm laser excitation. The full width at half maximum of the bandpasses is represented to indicate the range of wavelength collected for the luminescence measurements.

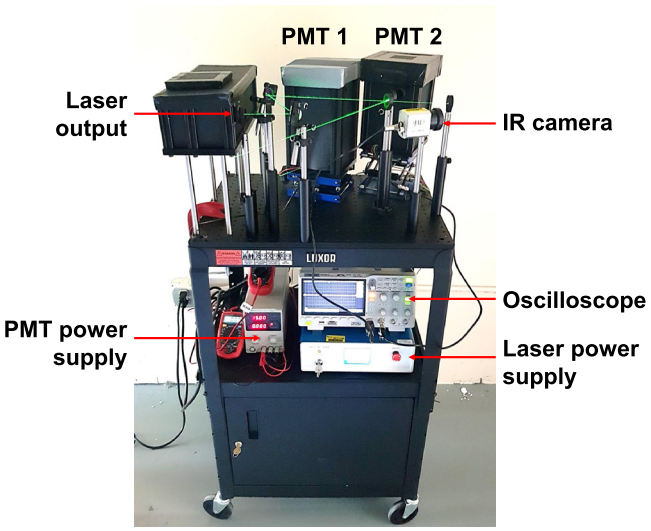

Figure 3. Overall view of the phosphor thermometry instrumentation.

optical breadboard. The phosphor thermometry instrumentation is equipped with a YAG:Nd pulsed laser (CNI) that provides 10 ns of laser output at a frequency of 10 Hz. The radiation emitted by the laser head is the fundamental mode at 1064 nm with an pulse energy of approximately 2 mJ. Firstly, it travels through a frequency-doubling KTP crystal to generate 532 nm pulses on the order of 0.5–1 mJ. Secondly, the 1064 nm and 532 nm beams are collinearly traveling through an LBO crystal to generate pulses at the sum frequency of 355 nm, with pulse energies up to 0.5 mJ. The PMTs are two Hamamatsu R3896s powered by a single precision direct current power supply providing 15 V and a maximum current of 90 mA for each detector. The maximum internal resistance of the gain control module of each PMT was measured to be around 80 kΩ.

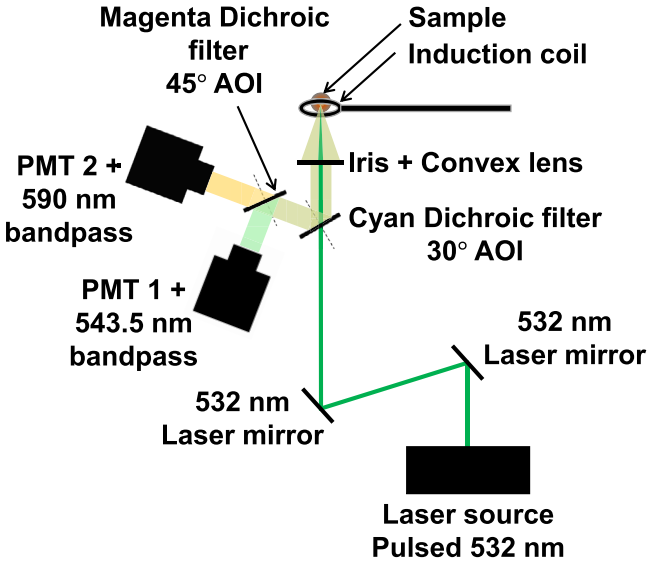

Figure 4. Phosphor thermometry instrumentation for the synchronized monitoring of luminescence from YSZ:Er,Eu.

3.2. Optical setup

For this experiment, the 532 nm excitation was chosen and the 355 nm was stopped with a beam blocker. A couple of laser mirrors were used to adjust the direction of the beam to the sample. After the laser beam was correctly aligned in the axis of the sample, a cyan dichroic filter (FD1C—Thorlabs) was placed in the path of the beam so the angle of incidence (AOI) was 30°. This value was chosen as it lowers the reflection of the laser light on the dichroic filter and allows for a higher excitation intensity onto the sample. A magenta dichroic filter (FD1M—Thorlabs) was then placed with an angle of incidence of 45° from the axis of reflection of the cyan dichroic filter. This allowed the convoluted luminescence of the co-doped sample that was reflected on the cyan dichroic filter to be further split into two spectral bands. The shorter wavelengths containing the erbium emissions were reflected on the magenta dichroic filter and directed to PMT 1, located in the axis of reflection of the magenta dichroic filter. On the other hand, the longer wavelengths containing the europium emissions were transmitted through the magenta dichroic filter to PMT 2, located in the axis of reflection of the cyan dichroic filter. The distance from the cyan dichroic filter to the sample was approximately 30 cm and the distance between the two dichroic filters was approximately 8 cm. For the collection of the decays, the two PMTs were used simultaneously. On PMT 1, connected to the channel 1 of the oscilloscope, a 543.5 nm (10 nm FWHM—Thorlabs) bandpass was placed in the viewing port of the detector. Because the wavelengths of the erbium emission at 545 nm and the excitation at 532 nm are close to each other, some laser leakage occurred due to laser reflections passing though the bandpass, which has a transmission and optical density at 532 nm of 0.19% and 2.73, respectively. As the laser intensity is very high in comparison with the luminescence intensity, to better protect the PMT and avoid the undesired collection of laser light, a longpass filter with an optical density of 5 on the 190–532 nm range was added. On PMT 2, connected to the channel 2 of the oscilloscope, a 590 nm (10 nm FWHM—Thorlabs) was mounted in the viewing port. To avoid direct exposition to intense laser reflections, prevented by the collection of external light, and capture exclusively light traveling through the optical components of the instrument, a laser barrier panel was placed in front of the instrument. A viewing hole was extruded to insert an iris, opened to its maximum aperture (25 mm) and a 125 mm convex lens, which converges the slightly divergent laser beam onto the sample. This arrangement results in a spot size of about 4 mm on the surface of the sample, placed at the focal distance of the convex lens, and allows for the collimation of the luminescence light traveling to the detectors. The optical setup that was assembled for this study is presented in figure 4.

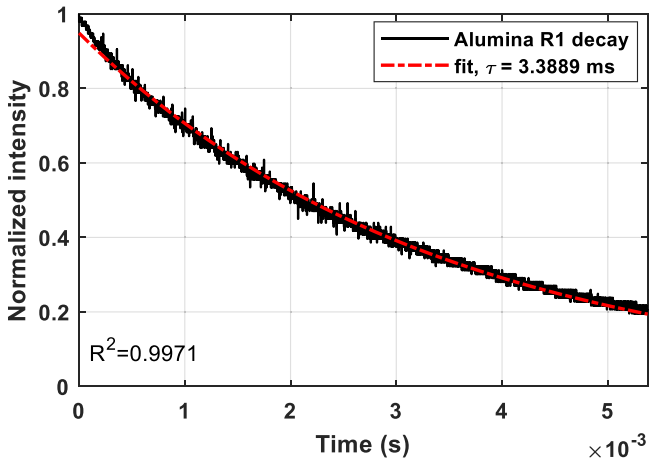

Figure 5. Room temperature decay of the R1-line of alumina.

3.3. Instrument initial test

The instrument was tested using the well-known R-line (ruby) emitted from an alumina block under a 532 nm excitation pulse. This experiment was achieved at room temperature and using a 694.3 nm bandpass (10 nm FWHM—Thorlabs) for the specific collection of the R1-line decay. A cyan dichroic filter (FD1C—Thorlabs) was used to transmit the laser beam to the sample and to reflect the luminescence signal to the detector. The resulting decay was fitted using a single-exponential model and is presented in figure 5. The obtained decay is comparable to values found in literature [27, 28].

3.4. High temperature setup

For this study, high temperature was achieved via induction heating (RDO HU2000), which produces the high frequency pulsating of magnetic fields to induce internal eddy currents in the material. These eddy currents begin to circulate, causing resistive heating within the material [29]. A frequency of 272 kHz and lift-off distance of 5 mm was used between the induction coil and the surface of the sample, as shown in figure 6(a). The resistive heating Q, generated by the internal eddy currents can be described by equation (1):

$$Q = \frac{1}{\sigma} \cdot |J_s|^2 \tag{1}$$

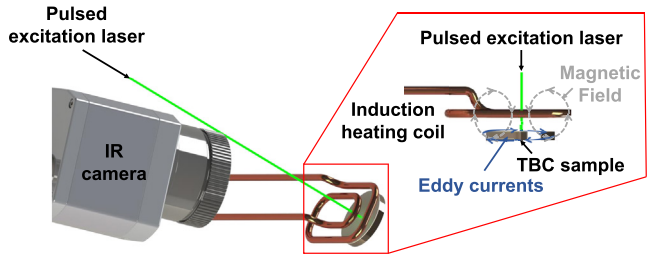

(a)

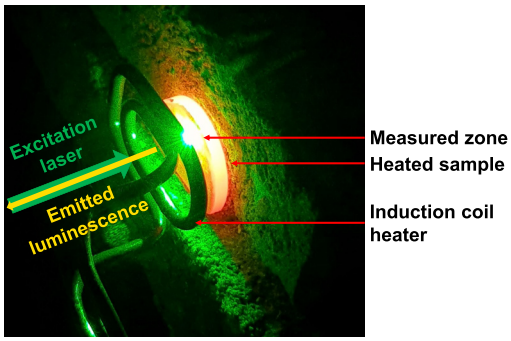

(b)

Figure 6. High temperature setup with (a) the induction system principle and temperature control using a long-wave infrared camera, (b) a view of the heated sample with the phosphor thermometry measurement.

where σ is equal to electrical conductivity and J_s is the eddy current density generated by the magnetic field. In order to keep the sample surface parallel to the induction coil and normal to the horizontal path of the laser beam, a circular segment of the disk was cut off so the sample can stand on refractory blocks, as shown in figure 6(b). Temperature increments of 50 °C were achieved up to 1100 °C through increasing the power of the inducting system and phosphor thermometry data was collected at each temperature step. Induction heating was chosen for this study as it does not produce background thermal radiation that facilitates luminescence measurements.

3.5. Control of the temperature using infrared thermometry

The temperature was measured using a TIM450 (Micro-Epsilon) longwave infrared camera (7–13 μm) operating at 30 Hz and placed at 20 cm from the sample, which corresponds to the focal distance of the camera. The collection area was reduced to match the phosphor thermometry laser spot size. The camera uses the program TIM Connect to track the thermal radiation emitted from the sample. The emissivity was set to $\epsilon = 0.95$ for all readings as this value corresponds to the emissivity of YSZ in the long-wave infrared range and does not vary noticeably with temperature [30–32].

3.6. Data collection

3.6.1. Acquisition of luminescence decays. The luminescence decays of the erbium emission at 545 nm and the europium

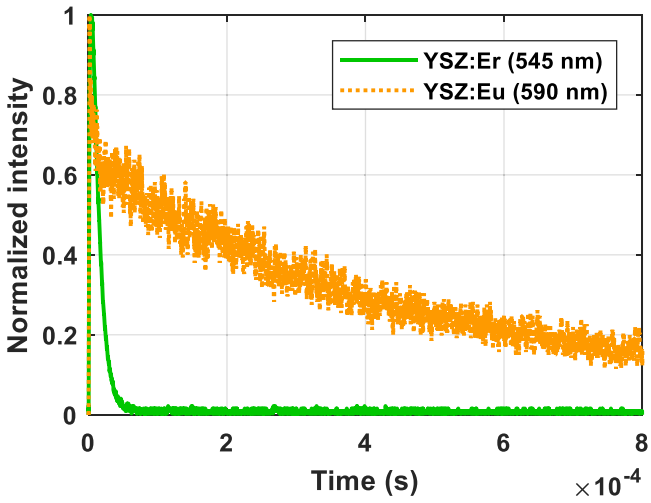

Figure 7. Synchronized collection of erbium and europium decays at 500 °C.

emission at 590 nm were captured simultaneously, using PMT 1 and PMT 2, respectively. A Siglent SDS 1204X-E oscilloscope was used to convert the electric signal to data matrices. In front of the viewing port of PMT 1, the incoming light is composed of a spectral band, which ranges in wavelength between 532 nm and 560 nm. It contains the luminescence emitted by erbium as well as some laser reflections. This light followed the optical path originating at the sample surface, reflected on the cyan dichroic filter with $R_{\text{cyan,545 nm}} \approx 95\%$ and reflected on the magenta dichroic filter with $R_{\text{magenta,545 nm}} \approx 92\%$. The spectral band was narrowed down to select the peak of erbium at 545 nm, using both a 543.5 nm bandpass and a laser cutoff longpass, as described in the optical setup section. Similarly, in front of PMT 2, the incoming signal contains a spectral band with a wavelength range between 560 nm and 720 nm. It contains the europium luminescence that emerges out of the sample surface and is reflected on the cyan dichroic filter with $R_{\text{cyan,590 nm}} \approx 100\%$ and transmitted through the magenta dichroic filter with $T_{\text{magenta,590 nm}} \approx 91\%$. The specific luminescence emission peak of europium at 590 nm was selected by placing the 590 nm bandpass described in the optical setup section in the viewing port of PMT 2. To obtain a greater amplitude of the signal that facilitates the detection of the luminescence decay and increases the signal-to-noise ratio (SNR), fixed resistance loads were connected to the RG58 coaxial cables that link the PMT detectors to the oscilloscope. Resistances of 50 kΩ and 5 kΩ were applied to the acquisition channels associated with PMT 1 for erbium and PMT 2 for europium, respectively. Figure 7 shows an example of the simultaneous decay acquisition, captured at 500 °C and showing the long decay of europium (≈632 μs) compared to the one oferbium (≈13 μs) as well as the higher noise of the europium decay due to the lower resistance value chosen for the acquisition. For this experiment, the amplitude of the signal was favored over time response to enable the use of luminescence intensities up to high temperature. By selecting these high feedthrough resistances, the minimum lifetime decay that could be accurately measured was found to be ≈6 μs for channel 1 and

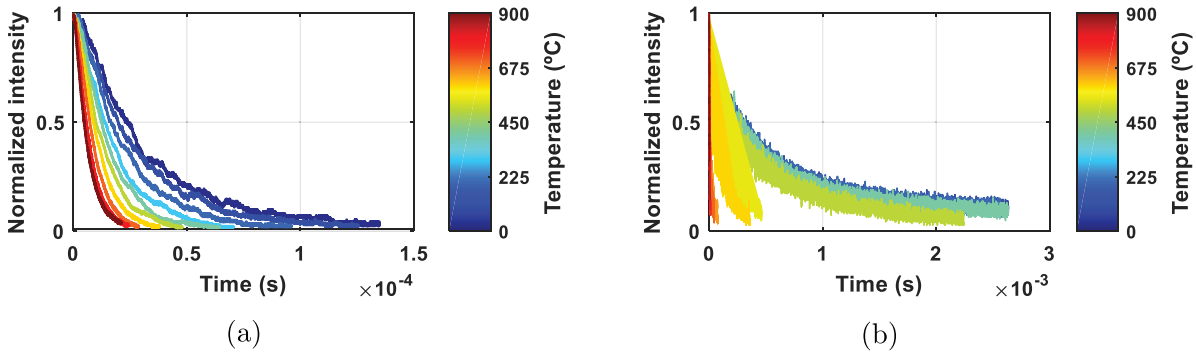

Figure 8. Behavior of the luminescence decays of (a) erbium and (b) europium with respect to temperature. (a) Er emission at 545 nm. (b) Eu emission at 590 nm.

≈1.5 μs for channel 2. After the completion of the experiment, the collected data was processed using a MATLAB code that synchronizes all decays so that $t = 0$ corresponds to the start of the decay at all temperatures, as presented in figure 8. The code uses a single exponential model to fit the data of both decays. Even though the europium decay has been shown to have a triple-exponential decay behavior [33], the single exponential model has been widely used as it offers a more robust fit for the temperature measurement using this phosphor [27, 34, 35].

3.6.2. Measurement of luminescence intensities. The use of two independent PMTs and high signal-to-noise ratio allows for the comparison of the intensities at $t = 0$, when the laser excitation pulse ends and where the luminescence intensity reaching the detectors is maximal. The PMTs receive a reduced region of the spectrum that is let through by the bandpasses and convert all the reaching photons to an electrical amplitude, measured in volts. The quantum efficiency of the PMTs is expected to be slightly higher at 545 nm (≈20%) than at 590 nm (≈18%). For this experiment, the feedthrough resistance of channel 1, which collects the luminescence of erbium, was set to a higher value than the one of channel 2, as it allowed to get amplitudes exceeding 1 V for both dopants. At room temperature, the integrated intensity of the luminescence of europium between 585 nm and 595 nm was found to be about 55% higher than the one of erbium between 538.5 nm and 548.5 nm (in the spectral ranges of the bandpasses). This is mainly due to the particular quantum yield of erbium and europium in YSZ, with the specific concentration and distribution parameters that were obtained for this sample. All the collected intensities were processed by the MATLAB routine to subtract the growing thermal radiation background from the measurements by averaging the intensity received by the PMTs when laser excitation is off and no luminescence remains. This takes place typically just before a new excitation pulse, which corresponds on the oscilloscope window to the trace preceding the rise-time and decay. The ratio between the normalized intensities of the two dopants can be used for high temperature measurements, assuming that the spectral shift due to temperature is negligible in comparison with the spectral bandpass of the filters used for the collection of light [36]. The integrated intensity measured by each of the two PMTs is, in consequence, assumed to remain proportional to the peak intensity of each radiative transition.

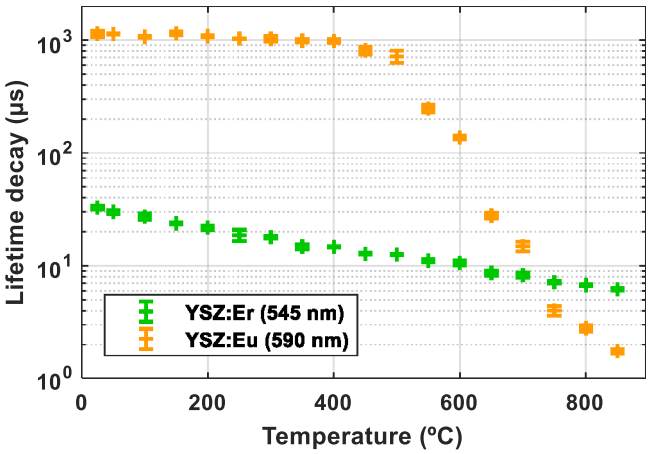

Figure 9. Lifetime decay response of APS co-doped YSZ:Er,Eu.

4. Results and discussions

4.1. Temporal analysis

The independent luminescence decays were fitted at each 50 °C step and the results were reported in figure 9. The error bars represent the standard deviation of three independent measurements that were performed with an identical setup, on three different locations onto the sample. It can be seen that the decay of erbium at 545 nm is sensitive to temperature over the entire range of temperature from room temperature to 850 °C with a lifetime decay time at room temperature of approximately 31 μs. The decay of europium has a very high sensitivity in the range of temperature comprised in between the quenching temperature of the phosphor in YSZ (≈500 °C) and 850 °C, with a lifetime decay time of approximately 1.2 ms at room temperature. The advantage of the co-doped configuration and simultaneous data acquisition of the decays is the extension of the temperature range on which the decay method is applicable as the individual dopants have different maximum sensitivity temperature ranges. Past 850 °C, the fits of the europium decay indicates a lifetime that stagnates around 1.5 μs that corresponds to the detection limit of the instrument on this channel, which is related to the resistance used for collection of the signal, as described in the data acquisition section. This temperature also matches with the limit found in literature for YSZ:Eu^{3+} [35, 37]. This inaccurate lifetime decay is generated by the limited response of

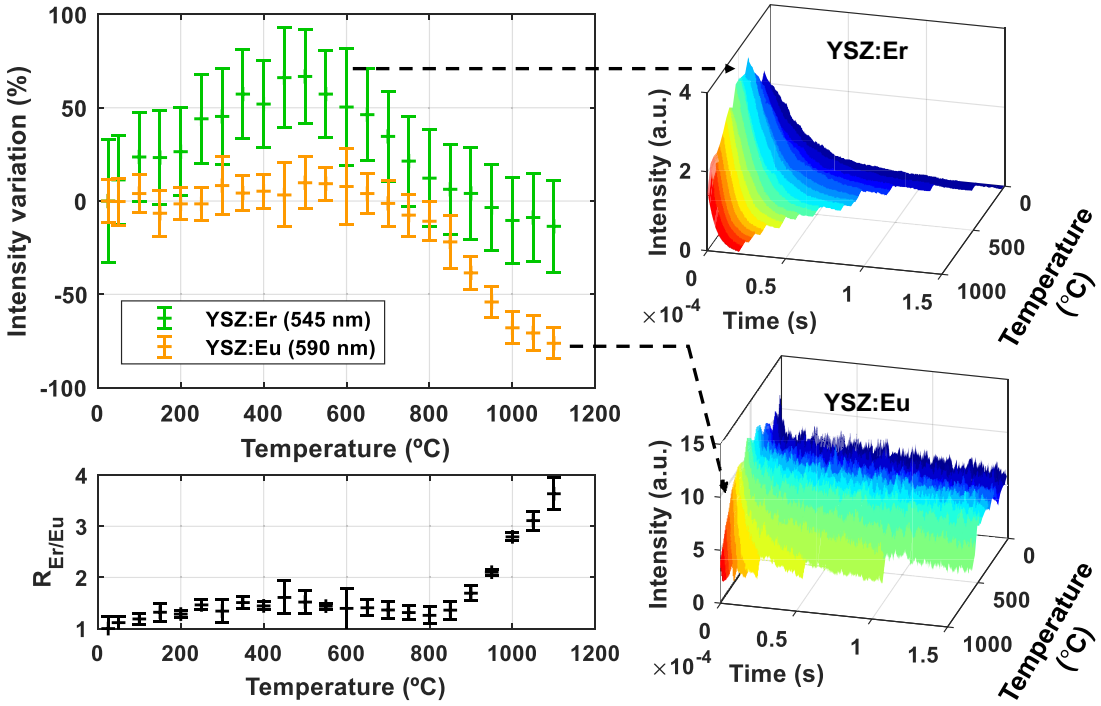

Figure 10. Percent luminescence intensity variation with respect to room temperature intensity for each dopant and corresponding ratio, sensitive between 850 °C and 1100 °C and usable for high temperature measurements.

the instrument at high temperature [38]. Reducing the resistance feedthrough on the channel can reduce the response time to some extent, but it implies a significant degradation of the SNR. A compromise between signal-to-noise ratio and time-resolution has to be selected for high temperature phosphor thermometry. The sensitivity of the decay of europium appears to be very high between 500 °C and 850 °C, which corresponds to the luminescence quenching of the dopant into YSZ, due to the higher probability of vibrational deexcitation past the quenching temperature. However, the sensitivity of the decay of europium outside this highly sensitive temperature range being close to zero. The combination of europium with erbium, facilitated by the instrument, allows for the extension of the range of temperature that can be measured using the decay method. This is because the lifetime decay of Erbium can be conveniently differentiated for any temperature between room temperature and the turbine system operating temperatures.

4.2. Intensity considerations

The luminescence intensity variation was measured and the ratio between the intensities of the erbium emission at 545 nm and the europium emission at 590 nm, normalized with respect to their distinct room temperature intensity. This data was obtained to provide additional information for the temperature measurement using the phosphor thermometry instrumentation. The luminescence intensity was obtained by measuring the maximum of the amplitude of the luminescence decay, which is proportional to the amount of photons reaching each PMT at the moment where the laser excitation pulse produces the strongest luminescence. As the temperature increases, it was found that the luminescence intensity of both dopants initially increased, due to the thermal filling of the energy levels, then decreased due to thermal quenching. The growing thermal radiation, which spectral radiance can be predicted using Planck's law, provides a contribution to the overall intensity of which one part is the luminescence. The percent variation of the luminescence intensity for each dopant, with respect to the room temperature intensity, is reported in figure 10. The error bars indicate the standard deviation of three independent measurements that were performed with an identical setup, on three different locations onto the sample. It was also found that the ratio of the normalized intensity variation of erbium to europium, $R_{\mathrm{Er/Eu}}$, has a sensitive range of temperature, usable from 850 °C up to at least 1100 °C, as presented in the lower plot. The error bars report the propagation of error from the ratio of the intensity variation between erbium and europium. This is a result of the fast quenching of europium luminescence on this range compared to the luminescence of erbium, which remains strong, as shown in the 3D plots. Although the lifetime decay of europium cannot be accurately determined past 850 °C due to the limitation on the temporal resolution of the instrument, the high SNR allows for valid intensity measurements at higher temperatures.

4.3. Measurement error considerations

To evaluate the precision and obtain a representative response of the instrument with the YSZ:Er,Eu sample, three independent measurements were performed. The phosphor thermometry instrumentation setup remained unchanged while the sample and the induction coil were translated normally to the laser to collect the luminescence signal from three different

locations. It is important to consider the intrinsic temperature measurement uncertainty implied by the utilization of infrared thermometry, whose accuracy is ±2% at high temperature. Indeed, the material was brought to the desired temperature values for data collection using infrared thermometry as the reference to determine the power input of induction heating. Another limiting factor when targeting a temperature for measurement is due to the gradient of temperature in the doped layer, created by the heat flux from the top surface to the bond coat in TBCs, but which direction is inverted in this study due to the utilization of the induction coil that preferentially heats the metallic substrate and dissipates heat by convection at the free surfaces of the material. Furthermore, material characteristics can vary importantly with the position probed on the sample. For example, the random distribution of porosity affecting both thermal and optical properties of the material and the irregularity of the doped layer thickness contribute in possible variations in the luminescence of the sample. A possible uneven distribution of dopant into the material, possibly intensifying ion–ion interaction, or the consecutive thermal cycling can also result in intensity and lifetime decay variation when probing different locations onto the doped layer. Uncertainty on the exponential fit can also be significant, in particular with europium, which typically exhibits a triple-exponential decay behavior. The precision of the measurements at 800 °C was found to be ±8 °C and ±3 °C, using erbium and europium decays, respectively. In addition, it can be noted that the current instrumentation is a lab-scale prototype that would necessitate automated acquisition for calibration to reduce experimental errors and that would require further development to allow for measurements on an operating engine, using an optical port, similar to other existing instrumentation [39].

5. Conclusions and perspectives

A phosphor thermometry instrument has been developed for the synchronized data collection of the luminescence decay and intensity ratio measured from two independent emission peaks coming from an erbium-europium co-doped yttria-stabilized zirconia air plasma spray thermal barrier coating. The luminescence emerging out of the doped layer was collected up to 1100 °C with 50 °C steps, while the surface temperature was concurrently measured using a longwave infrared camera. The high resistances at the input of the oscilloscope, chosen to amplify the signal-to-noise ratio, allowed us to collect lifetime decays with a sufficient bandwidth up to 850 °C. The results were found to be in good accordance with the literature. At higher temperatures, the limited response time was compensated by the acquisition of the ratio of intensity between erbium and europium emission peaks, which varies significantly due to the faster quenching of europium. As a consequence, the range of temperature that can be accurately measured using rare-earth doped YSZ configurations was extended up to turbine engine operating temperatures. The simultaneous acquisition of phosphor phermometry data achieved in this work paves the way for increased precision measurements on extended temperature ranges using the high-sensitivity decay method combined with the high-detectability intensity ratio method. Exploiting the synchronized acquisition capabilities of this novel phosphor thermometry instrumentation further will provide efficient *in-situ* temperature measurement options for turbine components.

Acknowledgments

The authors thank Mr Frank Accornero and Dr Mary McCay (Applied Research Laboratory, Florida Institute of Technology) for their support with the APS deposition and Dr Ramesh Subramanian (Siemens Energy) for providing the CM247 substrate that was used for the fabrication of the sample. This research is supported by the US Department of Energy, National Energy Technology Laboratory, University Turbine Systems Research (UTSR): DE-FE00312282.

ORCID iDs

Seetha Raghavan https://orcid.org/0000-0001-5389-9417

References

[1] Darolia R 2013 Thermal barrier coatings technology: critical review, progress update, remaining challenges and prospects *Int. Mater. Rev.* **58** 315–48
[2] Yañez Gonzalez A, Pilgrim C C, Feist J P, Sollazzo P Y, Beyrau F and Heyes A L 2015 On-line temperature measurement inside a thermal barrier sensor coating during engine operation *J. Turbomach.* **137** 101004
[3] Cheruvu N S, Chan K S and Viswanathan R 2006 Evaluation, degradation and life assessment of coatings for land based combustion turbines *Energy Mater.* **1** 33–47
[4] Manero A II, Selimov A, Fouliard Q, Knipe K, Wischek J, Meid C, Karlsson A M, Bartsch M and Raghavan S 2017 Piezospectroscopic evaluation and damage identification for thermal barrier coatings subjected to simulated engine environments *Surf. Coat. Technol.* **323** 30–8
[5] Manero A, Sofronsky S, Knipe K, Meid C, Wischek J, Okasinski J, Almer J, Karlsson A M, Raghavan S and Bartsch M 2015 Monitoring local strain in a thermal barrier coating system under thermal mechanical gas turbine operating conditions *J. Miner.* **67** 1528–39
[6] Feist J P, Heyes A L and Seefelt S 2003 Thermographic phosphor thermometry for film cooling studies in gas turbine combustors *Proc. Inst. Mech. Eng. A* **217** 193–200
[7] Copin E, Le Maoult Y, Sentenac T, Blas F, Tran T H G and Lours P 2014 Comparison of IR thermography and reflectance-enhanced photoluminescence for early quantitative diagnostic of thermal barrier coatings spallation *12th Int. Conf. on Quantitative InfraRed Thermography (QIRT 2014)* (Bordeaux, 07–11 July 2014)
[8] Allison S W and Gillies G T 1997 Remote thermometry with thermographic phosphors: instrumentation and applications *Rev. Sci. Instrum.* **68** 2615–50
[9] Eldridge J I *et al* 2004 Depth-penetrating temperature measurements of thermal barrier coatings incorporating thermographic phosphors *J. Thermal Spray Technol.* **13** 44–50
[10] Feist J P, Heyes A L, Choy K L and Su B 1999 Phosphor thermometry for high temperature gas turbine applications

ICIASF 99. 18th Int. Congress on Instrumentation in Aerospace Simulation Facilities (IEEE) pp 1–6
[11] Heyes A L, Feist J P, Chen X, Mutasim Z and Nicholls J R 2008 Optical nondestructive condition monitoring of thermal barrier coatings *J. Eng. Gas Turbines Power* **130** 061301
[12] Gonzalez A Y, Pilgrim C C, Sollazzo P Y, Heyes A L, Feist J P, Nicholls J R and Beyrau F 2014 Temperature sensing inside thermal barrier coatings using phosphor thermometry *Proc. Int. Instrumentation Symp.* (https://doi.org/10.1049/cp.2014.0540)
[13] Chen X, Mutasim Z, Price J, Feist J P, Heyes A L and Seefeldt S 2005 Industrial sensor TBCS: studies on temperature detection and durability *Int. J. Appl. Ceram. Technol.* **2** 414–21
[14] Nicholls J R, Wellman R G, Steenbakker R and Feist J 2010 Self diagnostic eb-pvd thermal barrier coatings *Advances in Science and Technology* vol 72 (Zurich: Trans Tech Publications) pp 65–74
[15] Eldridge J I, Bencic T J, Spuckler C M, Singh J and Wolfe D E 2006 Delamination-indicating thermal barrier coatings using YSZ: Eu sublayers *J. Am. Ceram. Soc.* **89** 3246–51
[16] Chambers M D and Clarke D R 2006 Effect of long term, high temperature aging on luminescence from Eu-doped YSZ thermal barrier coatings *Surf. Coat. Technol.* **201** 3942–6
[17] Eldridge J I and Wolfe D E 2019 Monitoring thermal barrier coating delamination progression by upconversion luminescence imaging *Surf. Coat. Technol.* **378** 124923
[18] Shen Y, Chambers M D and Clarke D R 2008 Effects of dopants and excitation wavelength on the temperature sensing of Ln^{3+}-doped 7YSZ *Surf. Coat. Technol.* **203** 456–60
[19] Amiel S, Copin E, Sentenac T, Lours P and Le Maoult Y 2018 On the thermal sensitivity and resolution of a YSZ: Er3+/YSZ: Eu3+ fluorescent thermal history sensor *Sens. Actuators* A **272** 42–52
[20] Gentleman M M and Clarke D R 2004 Concepts for luminescence sensing of thermal barrier coatings *Surf. Coat. Technol.* **188** 93–100
[21] Copin E B, Massol X, Amiel S, Sentenac T, Le Maoult Y and Lours P 2016 Novel erbia-yttria co-doped zirconia fluorescent thermal history sensor *Smart Mater. Struct.* **26** 015001
[22] Rabasović M D, Murić B D, Čelebonović V, Mitrić M, Jelenković B M and Nikolić M G 2016 Luminescence thermometry via the two-dopant intensity ratio of Y_2O_3: Er3+, Eu3+ *J. Phys. D: Appl. Phys.* **49** 485104
[23] Fuhrmann N, Brübach J and Dreizler A 2013 Phosphor thermometry: a comparison of the luminescence lifetime and the intensity ratio approach *Proc. Combust. Inst.* **34** 3611–8
[24] Brübach J, Pflitsch C, Dreizler A and Atakan B 2013 On surface temperature measurements with thermographic phosphors: a review *Prog. Energy Combust. Sci.* **39** 37–60
[25] Fouliard Q, Haldar S, Ghosh R and Raghavan S 2019 Modeling luminescence behavior for phosphor thermometry applied to doped thermal barrier coating configurations *Appl. Opt.* **58** D68–75
[26] Steenbakker R J L, Feist J P, Wellman R G and Nicholls J R 2009 Sensor thermal barrier coatings: remote *in situ* condition monitoring of EB-PVD coatings at elevated temperatures *J. Eng. Gas Turbines Power* **131** 041301
[27] Chambers M D and Clarke D R 2009 Doped oxides for high-temperature luminescence and lifetime thermometry *Annu. Rev. Mater. Res.* **39** 325–59
[28] Seat H C and Sharp J H 2004 Dedicated temperature sensing with c-axis oriented single-crystal ruby (Cr^{3+}: Al_2O_3) fibers: temperature and strain dependences of r-line fluorescence *IEEE Trans. Instrum. Meas.* **53** 140–54
[29] Davies J 1990 *Conduction and Induction Heating* vol 11 (London: Peter Pelegrinus Ltd)
[30] González-Fernández L, Del Campo L, Pérez-Sáez R B and Tello M J 2012 Normal spectral emittance of inconel 718 aeronautical alloy coated with yttria stabilized zirconia films *J. Alloys Compd.* **513** 101–6
[31] Markham J R and Kinsella K 1998 Thermal radiative properties and temperature measurement from turbine coatings *Int. J. Thermophys.* **19** 537–45
[32] Manara J *et al* 2017 Long wavelength infrared radiation thermometry for non-contact temperature measurements in gas turbines *Infrared Phys. Technol.* **80** 120–30
[33] Heeg B and Jenkins T P 2013 Precision and accuracy of luminescence lifetime-based phosphor thermometry: a case study of Eu (III): YSZ. *AIP Conf. Proc.* **1552** 885–90
[34] Yang L, Peng D, Zhao C, Xing C, Guo F, Yao Z, Liu Y, Zhao X and Xiao P 2017 Evaluation of the in-depth temperature sensing performance of Eu-and Dy-doped YSZ in air plasma sprayed thermal barrier coatings *Surf. Coat. Technol.* **316** 210–8
[35] Shen Y and Clarke D R 2009 Effects of reducing atmosphere on the luminescence of Eu3+-doped yttria-stabilized zirconia sensor layers in thermal barrier coatings *J. Am. Ceram. Soc.* **92** 125–9
[36] Kusama H, Sovers O J and Yoshioka T 1976 Line shift method for phosphor temperature measurements *Japan. J. Appl. Phys.* **15** 2349
[37] Feist J P and Heyes A L 2000 Europium-doped yttria-stabilized zirconia for high-temperature phosphor thermometry *Proc. Inst. Mech. Eng. L* **214** 7–12
[38] Cai T, Li Y, Guo S, Peng D, Zhao X and Liu Y 2019 Pressure effect on phosphor thermometry using Mg_4FGeO_6:Mn *Meas. Sci. Technol.* **30** 027001
[39] Feist J P, Sollazzo P Y, Berthier S, Charnley B and Wells J 2012 Precision temperature detection using a phosphorescence sensor coating system on a rolls-royce viper engine *ASME Turbo Expo 2012: Turbine Technical Conf. and Exposition* (American Society of Mechanical Engineers) pp 917–26